4*d*-5*p* Orbital Mixing and Asymmetric In 4*d*–O 2*p* Hybridization in $InMnO_3$: A New Bonding Mechanism for Hexagonal Ferroelectricity

Min-Ae Oak,[1] Jung-Hoon Lee,[1] Hyun Myung Jang,[1,2,*] Jung Suk Goh,[3] Hyoung Joon Choi,[3] and James F. Scott[4]

[1]*Department of Materials Science and Engineering, and Division of Advanced Materials Science, Pohang University of Science and Technology (POSTECH), Pohang 790-784, Republic of Korea*

[2]*Department of Physics, Pohang University of Science and Technology (POSTECH), Pohang 790-784, Republic of Korea*

[3]*Department of Physics and IPAP, Yonsei University, Seoul 120-749, Republic of Korea*

[4]*Department of Physics, Cavendish Laboratory, University of Cambridge, Cambridge CB3 0HE, United Kingdom*

(Received 11 September 2010; published 24 January 2011)

Recent studies on the ferroelectricity origin of $YMnO_3$, a prototype of hexagonal manganites (*h*-*R*MnO_3, where *R* is a rare-earth-metal element), reveal that the d^0-ness of a Y^{3+} ion with an anisotropic Y 4*d*–O 2*p* hybridization is the main driving force of ferroelectricity. $InMnO_3$ (IMO) also belongs to the *h*-*R*MnO_3 family. However, the d^0-ness-driven ferroelectricity cannot be expected because the trivalent In ion is characterized by a fully filled 4*d* orbital. Here we propose a new bonding mechanism of the hexagonal ferroelectricity in IMO: intra-atomic $4d_{z^2}$-$5p_z$ orbital mixing of In followed by asymmetric $4d_{z^2}$(In)–$2p_z$(O) covalent bonding along the *c* axis.

DOI: 10.1103/PhysRevLett.106.047601 PACS numbers: 77.84.−s, 71.15.Mb, 71.20.−b, 75.50.Ee

Multiferroic materials have received a great deal of attention because of their potential for enabling entirely new device paradigms [1–6]. Among these, manganite-based multiferroics have been the most extensively studied. Orthorhombic manganites such as $TbMnO_3$ [2] and $TbMn_2O_5$ [3] exhibit a strong tendency of the magnetoelectric coupling which stems from a noncollinear spin-ordering-induced improper or pseudoproper ferroelectricity [6,7]. In hexagonal manganites (*h*-*R*MnO_3, where *R* is a rare-earth-metal element), on the other hand, an asymmetric movement of *R* ions from the centrosymmetric position is known to be a prevailing factor in the manifestation of ferroelectricity [8,9].

Among hexagonal manganites, $YMnO_3$ is a prototype of the *h*-*R*MnO_3 family and is currently being extensively investigated. However, there have been some conflicting reports on the nature of ferroelectricity in $YMnO_3$ (YMO). According to a pioneering work by Van Aken *et al.* [9], the ferroelectric transition to the $P6_3cm$ symmetry is driven entirely by electrostatic and size effects which are accompanied by an off-centering displacement of Y ions. Thus, they concluded that the Y-O bonds are predominantly ionic and orbital hybridization, thus, covalency plays a minor role in this displacive transition [9]. However, more recent studies all reveal that the d^0-ness of a Y^{3+} ion ($4d^0$) with a strong hybridization with the O 2*p* orbital is the main driving force of the hexagonal ferroelectricity [10–12].

Considering the ferroelectricity driven by Y d^0-ness in YMO [10,11], it is of great scientific importance to clearly elucidate the role of d^0-ness in other types of hexagonal manganites. $InMnO_3$ (IMO) also belongs to the *h*-*R*MnO_3 family [13,14], and Fe-substituted IMO-based perovskites were recently proposed as a promising new class of near-room-temperature multiferroics [15]. In the case of IMO, however, the d^0-ness-driven ferroelectricity cannot be expected because the trivalent In ion which is expected to be responsible for the ferroelectricity is characterized by a fully filled 4*d* electronic structure, namely, (Kr core) $4d^{10}$. Reflecting this puzzling situation, there have been some conflicting reports on the dielectric nature of the hexagonal IMO, namely, ferroelectricity [16] versus paraelectricity [17]. In view of the this dilemma in the electronic origin of ferroelectricity, it is of great scientific importance to elucidate the main driving force of the ferroelectricity in IMO. On the basis of first-principles calculations [18], we propose a new bonding mechanism of the hexagonal $P6_3cm$ ferroelectricity: intra-atomic $4d_{z^2}$-$5p_z$ orbital self-mixing of In followed by asymmetric $4d_{z^2}$(In)–$2p_z$(O) hybridization along the *c* axis of IMO.

In Fig. 1(a), we compare the optimized crystal structure of the ferroelectric $P6_3cm$ unit cell with that of the paraelectric $P6_3/mmc$ cell. Similar to YMO, the two hexagonal structures commonly share (i) the InO_8 unit having trigonal D_{3d} site symmetry and (ii) the MnO_5 bipyramid with D_{3h} site symmetry. As shown in Fig. 1(b), there exist two different types of oxygen ions surrounding the central In ion in the InO_8 unit: two apical (axial) oxygen ions along the hexagonal *c* axis (abbreviated as O_A) and six oxygen ions located at two different triangular in planes (abbreviated as O_I). Notice that O_A and O_I are equivalent to O_P (in-plane oxygen) and O_T (on-top oxygen), respectively, in the MnO_5 bipyramidal unit [9,10]. The main difference between these two structures is that, in the paraelectric $P6_3/mmc$ phase, all ions are constrained to planes that are parallel to the *a*-*b* plane, whereas the mirror planes perpendicular to the *c* axis disappear in the ferroelectric $P6_3cm$ phase.

The computed local structure reveals that the ferroelectricity originates from the vertical shift of the In ion in the InO_8 unit from the centrosymmetric position [18]. In addition, IMO possesses three distinct In-ion sites in the ferroelectric state. Among these, the first two dipoles are parallel to each other but are antiparallel to the third remaining dipole (a ferroelectric nature). Thus, the net polarization is parallel to the c axis of $P6_3cm$, as depicted in Fig. 1(b). On the other hand, the net off-centering distortion in the MnO_5 unit is negligible [18], indicating that the MnO_5 unit is not responsible for the manifestation of the ferroelectricity.

According to the computed double-well potential [Fig. 1(c)], the barrier height for the dipole switching along the c axis is 0.438 eV per unit cell. This clearly demonstrates the thermodynamic stability of the ferroelectric $P6_3cm$ phase over the centrosymmetric $P6_3/mmc$ phase. We also have examined the thermodynamic stability of other possible intermediate phases: paraelectric $P6_3/mcm$ and ferroelectric $P6_3mc$ phases [19]. The total Kohn-Sham (KS) energy calculations indicate that the ferroelectric $P6_3cm$ phase is substantially more stable than these phases. According to our density-functional theory (DFT) calculations, the equilibrium off-center displacement of the In ion along the c axis is antiparallel to that of the O_A ion but with the same displacement of 0.284 Å [18]. This indicates that the net off-centering distortion is 0.568 Å. The ferroelectric polarization evaluated by applying the Berry-phase method [20] is 4.43 $\mu C/cm^2$.

It is of scientific importance to examine the role of spin ordering in stabilizing the ferroelectric phase. For this purpose, we adopted a suitable noncollinear triangular antiferromagnetic (AFM) spin configuration which had been originally proposed by Katsufuji and co-workers [21]. This configuration is schematically depicted in Fig. 1(d). According to the total KS energy calculations of the ferroelectric $P6_3cm$ phase, the AFM spin ordering greatly stabilizes the ferroelectric phase with the KS energy reduction of 3.0 eV per formula cell. On the contrary, the ferroelectric dipole ordering only reduces the KS energy by 0.073 eV per formula cell (i.e., 0.438 eV per unit cell) for a given ordered spin configuration [18]. Thus, it can be concluded that the triangular AFM spin ordering is necessary for the stabilization of the ferroelectric $P6_3cm$ phase relative to the paraelectric $P6_3/mmc$ phase.

Let us now examine the main issue of the present study, namely, the electronic origin of the hexagonal ferroelectricity. For this purpose, we first compare the computed electron localization function (ELF) of the $P6_3cm$ phase with that of the paraelectric $P6_3/mmc$ phase since the ELF is known to be an informative tool to distinguish different bonding interactions in solids [22,23]. As shown in Fig. 2, the ELF value between the In ion and the axial O_A is negligible in the paraelectric $P6_3/mmc$ state, which demonstrates a dominant ionic bonding character in the In-O_A bond. It is interesting to notice that upon the transition

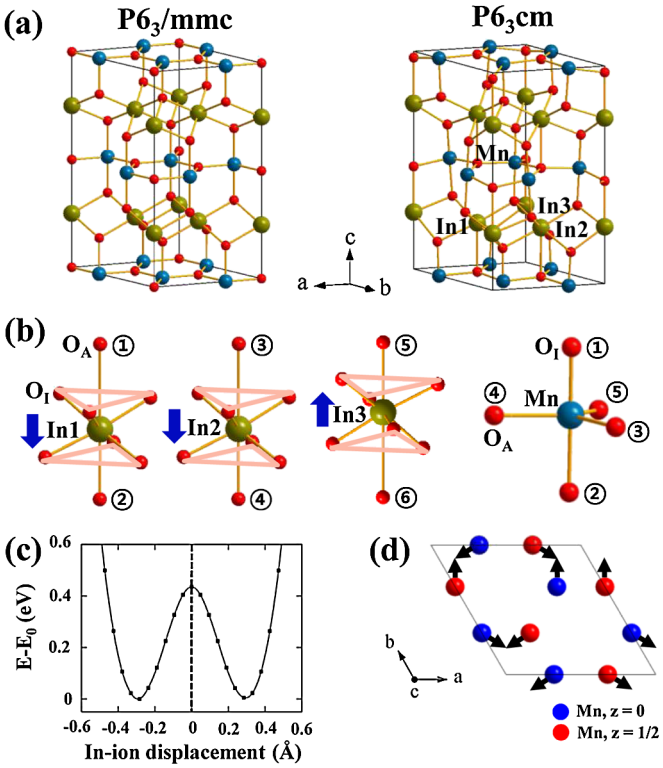

FIG. 1 (color online). Crystal, off-centering, and spin structures of $InMnO_3$. (a) Two polymorphic crystal structures of the hexagonal $InMnO_3$ (IMO): paraelectric $P6_3/mmc$ structure (left) and ferroelectric $P6_3cm$ structure (right). (b) The three distinct InO_8 units and the MnO_5 bipyramidal unit in the ferroelectric state. The three blue arrows indicate the direction of the off-centering displacement in each InO_8 unit. (c) The computed double-well potential plotted as a function of the In-ion displacement from the centrosymmetric position. (d) A schematic representation of the noncollinear triangular antiferromagnetic spin configuration adopted in our DFT calculations. Here the arrows at the blue Mn ions denote the directions of the Mn-magnetic moments on the a-b plane at $z = 0$ while the arrows at the red Mn ions represent the directions on the a-b plane at $z = 1/2$.

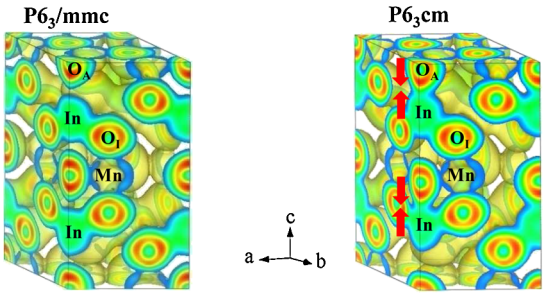

FIG. 2 (color online). A comparison of the three-dimensional ELF contour of the paraelectric $P6_3/mmc$ phase with that of the ferroelectric $P6_3cm$ phase. The isosurface level is equal to 0.07 $e/Å^3$.

to the ferroelectric $P6_3cm$ phase, the In ion moves to an asymmetric position and there occurs a strong covalent-bonding interaction between the In ion and one of the two O_A ions along the c axis. This results in a spontaneous breaking of the centrosymmetric state, as marked with red arrows in Fig. 2. The difference in the ELF between the ferroelectric state and the paraelectric state [defined as δELF(**r**)] introduced by Stroppa *et al.* [23] also demonstrates a strong asymmetric electron localization along the c axis upon the transition to the ferroelectric $P6_3cm$ state [18]. On the contrary, there is no noticeable change in the computed ELF for both In-O_I and Mn-O_I bonds. This suggests that the asymmetric In-O_A bonding interaction is mainly responsible for the paraelectric-to-ferroelectric transition. Our ELF results of YMO [18] indicate that the Y $4d$–O $2p$ hybridization is substantially weaker than the present In $4d$–O $2p$ hybridization.

Having demonstrated a strong In-O_A bonding interaction associated with the transition to the $P6_3cm$ state, we now address the following important point: What kinds of orbital interactions are involved in the asymmetric In-O_A covalent bonding? To answer this question, we have carefully examined partial density of states (PDOS) for various atomic orbitals involved in the bonding interaction. In Fig. 3(a), we compare the orbital-resolved PDOS for In $4d$, O_A $2p$, and Mn $3d$ of the paraelectric $P6_3/mmc$ phase with those of the ferroelectric $P6_3cm$ phase. The two prominent differences in the PDOS between these two phases are (i) a remarkable enhancement of the $4d_{z^2}$-orbital PDOS of In (for a wide energy range between -2.5 and 0 eV below the valence top) upon the transition to the ferroelectric state and (ii) a strong overlapping of the In $4d_{z^2}$-orbital PDOS with the apical O_A $2p_z$-orbital PDOS. Because of the antisymmetric nature of the $2p_z$ orbital wave function along the z direction, the In $4d_{z^2}$–O_A $2p_z$ orbital overlapping is symmetry allowed only for one neighboring In-O_A bond. As a result of this asymmetric overlapping, the In atom in an InO_8 cage cannot undergo a simultaneous symmetric bonding interaction with the two neighboring O_A atoms. This asymmetric In $4d_{z^2}$–O_A $2p_z$ hybridization leads to an off-centering ferroelectric distortion along the c axis.

Though the PDOS and ELF results indicate a strong In $4d_{z^2}$–O_A $2p_z$ hybridization, we still have one puzzling question associated with this hybridization since the d^0-ness-driven ferroelectricity cannot be expected in a fully filled $4d$ orbital of In, as mentioned previously. It is known that a half filled Fe^{3+} ion in $BiFeO_3$ undergoes a strong intra-atomic $3d$-$4p$ orbital mixing and the degree of this orbital self-mixing enhances with the ferroelectric distortion [24]. On the basis of this, we propose that the symmetry-allowed In $4d_{z^2}$-$5p_z$ orbital self-mixing enhances with the off-centering displacement. As presented in Fig. 3(b), the overlapping of the $4d_{z^2}$-orbital band with the $5p_z$-orbital band over the Γ-M first Brillouin zone is much more pronounced in the ferroelectric $P6_3cm$ state, showing the validity of this proposition.

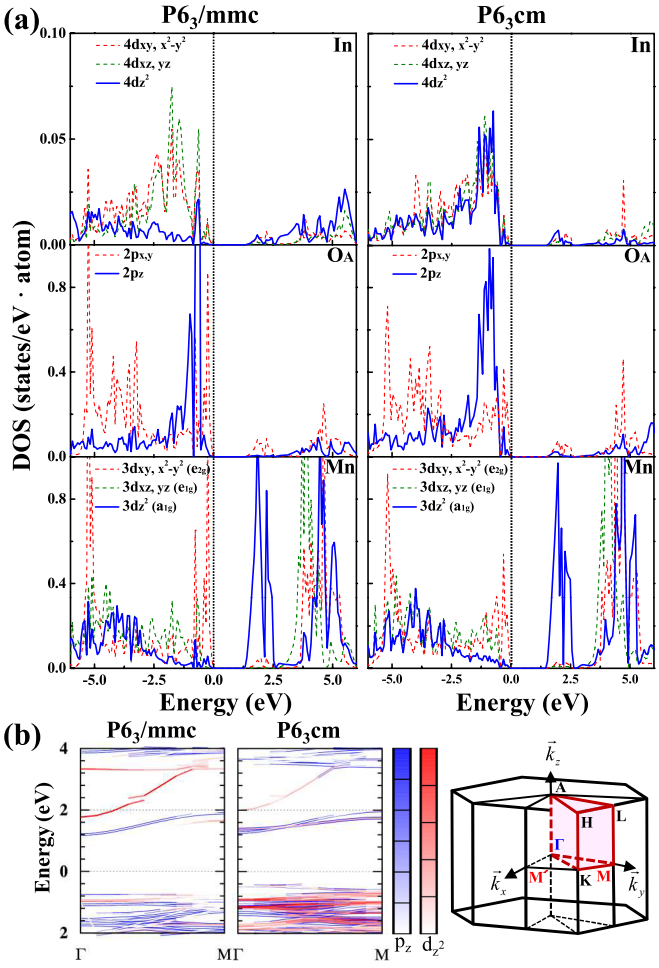

FIG. 3 (color online). (a) A comparison of the orbital-resolved partial density of states for In $4d$, O_A $2p$, and Mn $3d$ of the paraelectric $P6_3/mmc$ phase with those of the ferroelectric $P6_3cm$ phase. (b) In the two left-hand-side figures, the band structure of the paraelectric $P6_3/mmc$ phase is compared with that of the ferroelectric $P6_3cm$ phase for selected $4d_{z^2}$- and $5p_z$-orbital bands over the Γ-M first Brillouin zone. In the diagrams, a gradation of the line intensity was introduced to best represent the occupation density of each orbital over the Brillouin zone. Symmetry points and axes of the fist Brillouin zone of the hexagonal lattice are shown in the right-hand-side figure. Here M corresponds to the zone boundary point at which the three components of the wave vector are $(2\pi/a)(010)$.

The overlapping, however, produces a mixed orbital ($\phi_m = c_d\phi_{4d_{z^2}} + c_p\phi_{5p_z}$) with an asymmetric shape along the z direction (Fig. 4). Thus, the In atom with a self-mixed $4d_{z^2}$-$5p_z$ orbital is now able to make an asymmetric covalent bond with one of the two neighboring O_A ions (not simultaneously with two neighboring O_A ions), which results in a spontaneous breaking of the centrosymmetric state (Fig. 4). In view of this, the asymmetry in the mixed orbital wave function (ϕ_m) is the electronic origin

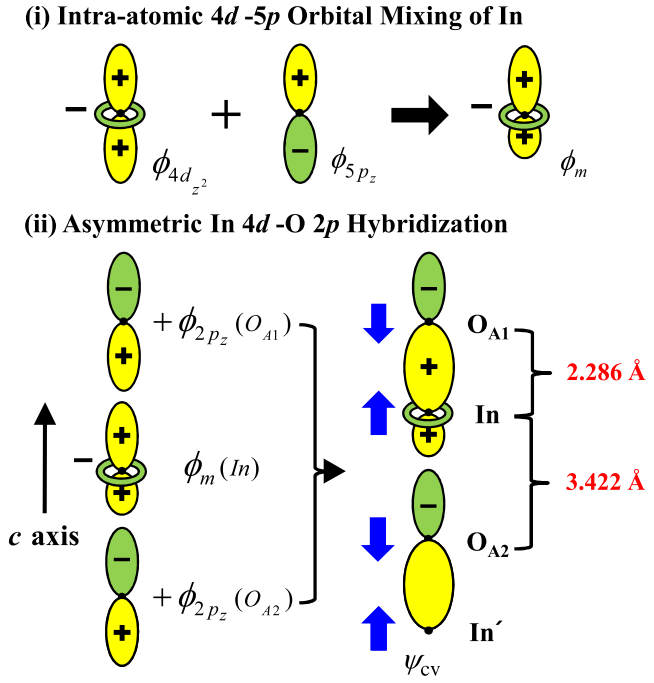

FIG. 4 (color online). Orbital interaction diagrams that illustrate a sequential bonding mechanism of the hexagonal ferroelectricity.

of the c-axis-oriented ferroelectricity. This mixed orbital is then capable of hybridizing with the two $2p_z$ orbitals of the apical oxygens, O_{A1} and O_{A2}. The hybridization results in a bonding molecular orbital (ψ_{cv}) for the asymmetric covalent interaction between In and O_A atoms, namely, $\psi_{cv} = \psi_{pd-p} = c_1\phi_{m(p_z)}(\mathrm{In}) + (c_2/\sqrt{2})\{\phi_{2p_z}(O_{A1}) + \phi_{2p_z}(O_{A2})\}$ [18]. Thus, a strong asymmetric covalent bonding between In and O_A atoms, thus, an off-centering ferroelectric polarization along the c axis (Fig. 2), can be explained by the following sequential mechanism (Fig. 4): (i) intra-atomic $4d_{z^2}$-$5p_z$ orbital mixing of In and (ii) asymmetric $4d_{z^2}(\mathrm{In})$–$2p_z(\mathrm{O})$ hybridization.

In conclusion, we proposed a new covalent-bonding mechanism of the hexagonal ferroelectricity in $InMnO_3$: intra-atomic $4d_{z^2}$-$5p_z$ orbital mixing of In followed by asymmetric $4d_{z^2}(\mathrm{In})$–$2p_z(\mathrm{O})$ covalent-bonding interaction along the c axis.

This work was financially supported by the WCU (World Class University) program funded by the Ministry of Education, Science and Technology of Korea (Grant No. R31-2008-000-10059-0).

*hmjang@postech.ac.kr

[1] J. Wang *et al.*, Science **299**, 1719 (2003).
[2] T. Kimura *et al.*, Nature (London) **426**, 55 (2003).
[3] N. Hur *et al.*, Nature (London) **429**, 392 (2004).
[4] T. Lottermoser *et al.*, Nature (London) **430**, 541 (2004).
[5] W. Eerenstein, N. D. Mathur, and J. F. Scott, Nature (London) **442**, 759 (2006).
[6] S.-W. Cheong and M. Mostovoy, Nature Mater. **6**, 13 (2007).
[7] P. Tolédano, Phys. Rev. B **79**, 094416 (2009); P. Tolédano, W. Schranz, and G. Krexner, *ibid.* **79**, 144103 (2009).
[8] C.-Y. Ren, Phys. Rev. B **79**, 125113 (2009).
[9] B. B. Van Aken, T. T. M. Palstra, A. Filippetti, and N. A. Spaldin, Nature Mater. **3**, 164 (2004).
[10] D.-Y. Cho *et al.*, Phys. Rev. Lett. **98**, 217601 (2007).
[11] C. Zhong, Q. Jiang, H. Zhang, and X. Jiang, Appl. Phys. Lett. **94**, 224107 (2009).
[12] J. Kim, K. C. Cho, Y. M. Koo, K. P. Hong, and N. Shin, Appl. Phys. Lett. **95**, 132901 (2009).
[13] D. M. Giaquinta and H. C. zur Loye, J. Am. Chem. Soc. **114**, 10 952 (1992).
[14] J. E. Greedan, M. Bieringer, J. F. Britten, D. M. Giaquinta, and H. C. zur Loye, J. Solid State Chem. **116**, 118 (1995).
[15] A. A. Belik, T. Furubayashi, Y. Matsushita, M. Tanaka, S. Hishita, and E. Takayama-Muromachi, Angew. Chem., Int. Ed. **48**, 6117 (2009).
[16] C. R. Serrao *et al.*, J. Appl. Phys. **100**, 076104 (2006).
[17] A. A. Belik *et al.*, Phys. Rev. B **79**, 054411 (2009).
[18] See supplemental material at http://link.aps.org/supplemental/10.1103/PhysRevLett.106.047601 for (i) spin-structure-dependent Kohn-Sham energy and (ii) molecular orbitals associated with In 4*d*–O 2*p* hybridization.
[19] C. J. Fennie and K. M. Rabe, Phys. Rev. B **72**, 100103(R) (2005).
[20] R. D. King-Smith and D. Vanderbilt, Phys. Rev. B **47**, 1651 (1993); D. Vanderbilt and R. D. King-Smith, *ibid.* **48**, 4442 (1993).
[21] T. Katsufuji *et al.*, Phys. Rev. B **66**, 134434 (2002).
[22] A. Savin, R. Nesper, S. Wengert, and T. F. Fässler, Angew. Chem., Int. Ed. **36**, 1808 (1997); P. Ravindran, R. Vidya, A. Kjekshus, H. Fjellvåg, and O. Eriksson, Phys. Rev. B **74**, 224412 (2006).
[23] A. Stroppa, M. Marsman, G. Kresse, and S. Picozzi, New J. Phys. **12**, 093026 (2010).
[24] J.-H. Lee *et al.*, Phys. Rev. B **82**, 045113 (2010).